International Journal of High-Rise Buildings
December 2021, Vol 10, No 4, 345-364
https://doi.org/10.21022/IJHRB.2021.10.4.345

International Journal of
High-Rise Buildings
www.ctbuh-korea.org/ijhrb/index.php

A Review and Analysis of the Thermal Exposure in Large Compartment Fire Experiments

Vinny Gupta[1,2], Juan P. Hidalgo[1], David Lange[1], Adam Cowlard[3], Cecilia Abecassis-Empis[3] and José L. Torero[4]

[1]*School of Civil Engineering, The University of Queensland, Australia*
[2]*Department of Aerospace, Mechanical and Mechatronics Engineering, The University of Sydney, Australia*
[3]*Torero, Abecassis Empis and Cowlard Ltd., United Kingdom*
[4]*Department of Civil, Environmental & Geomatic Engineering, University College London, United Kingdom*

Abstract

Developments in the understanding of fire behaviour for large open-plan spaces typical of tall buildings have been greatly outpaced by the rate at which these buildings are being constructed and their characteristics changed. Numerous high-profile fire-induced failures have highlighted the inadequacy of existing tools and standards for fire engineering when applied to highly-optimised modern tall buildings. With the continued increase in height and complexity of tall buildings, the risk to the occupants from fire-induced structural collapse increases, thus understanding the performance of complex structural systems under fire exposure is imperative. Therefore, an accurate representation of the design fire for open-plan compartments is required for the purposes of design. This will allow for knowledge-driven, quantifiable factors of safety to be used in the design of highly optimised modern tall buildings. In this paper, we review the state-of-the-art experimental research on large open-plan compartment fires from the past three decades. We have assimilated results collected from 37 large-scale compartment fire experiments of the open-plan type conducted from 1993 to 2019, covering a range of compartment and fuel characteristics. Spatial and temporal distributions of the heat fluxes imposed on compartment ceilings are estimated from the data. The complexity of the compartment fire dynamics is highlighted by the large differences in the data collected, which currently complicates the development of engineering tools based on physical models. Despite the large variability, this analysis shows that the orders of magnitude of the thermal exposure are defined by the ratio of flame spread and burnout front velocities (V_S / V_{BO}), which enables the grouping of open-plan compartment fires into three distinct modes of fire spread. Each mode is found to exhibit a characteristic order of magnitude and temporal distribution of thermal exposure. The results show that the magnitude of the thermal exposure for each mode are not consistent with existing performance-based design models, nevertheless, our analysis offers a new pathway for defining thermal exposure from realistic fire scenarios in large open-plan compartments.

Keywords: Compartment fires, Fire dynamics, Design fires, Travelling fires, Fire resistance

1. Introduction

The number of tall buildings in excess of 200 m constructed each year is increasing rapidly (Council on Tall Buildings and Urban Habitat 2021), more than doubling in the past decade. Development of these structures benefits significantly from optimisation and technological development in disciplines such as materials science, energy efficiency, structural and wind engineering. By contrast, fire engineering, and specifically structural fire engineering, has not advanced significantly since the development of the concept of fire resistance in the early 1900s (Law and Bisby 2020; Gales *et al.* 2021). Only recently, has our understanding of structural behaviour under fire conditions advanced considerably through the extensive modelling efforts of the British Steel Cardington Fire Tests within the "PIT Project", which highlighted how modern composite structures are "radically different from the present design philosophy" (The University of Edinburgh 2000, Sanad *et al.* 2000; Sanad *et al.* 2000; Gillie *et al.* 2001; Gillie *et al.* 2001). The result of this lack of development and innovation into our understanding of structural behaviour under thermal loading from fire has been marked by several high-profile fire-related failures such as the World Trade Center Towers 1, 2, 5 & 7 collapses (New York City, 2001) (Gann 2005), the Windsor Tower (Madrid, 2005) (Fletcher *et al.* 2007), Delft Technical University Department of Architecture partial collapses (Delft, 2008) (Engelhardt *et al.* 2013) and the Plasco Building fire (Tehran, 2017) (Behnam 2019; Ahmadi *et al.* 2020). These failures have demonstrated the need for greater knowledge development and improved, fully-validated fire engineered approaches when dealing with such optimised infrastructure.

†Corresponding author: Gupta, Vinny
Tel: +61-2-9351-2835
E-mail: vinny.gupta@sydney.edu.au

Life safety performance objectives of a tall building in a fire are determined based on the timescales of egress of the occupancy and the total duration of the fire. For tall buildings, the timescales associated with an evacuation are very long and often extend to the same order of magnitude as structural collapse or burnout of the fuel, thus the perception of risk to those occupants from structural collapse increases (Cowlard *et al.* 2013). It would be reasonable to expect that the timescale for structural failure must tend to infinity (i.e. no collapse), and this is the intent behind the concept of fire resistance (Law and Bisby 2020). Therefore, quantification of the structural response to the thermal exposure from the fire remains an unavoidable endeavour for a tall building design. Traditionally, this thermal exposure has been assumed to be consistent with the exposure and procedures embedded in the fire resistance framework.

The fire resistance framework generalises a natural fire into a standard time-temperature curve that can be used to establish durations of fire resistance for structural elements tested in isolation such that structural integrity and compartmentation could be maintained. Once the requirements for "fire resistance" are met for each structural element, it is assumed that the performance requirements for the structural system as a whole are all met, thereby disregarding the need to perform a structural analysis (Ingberg 1928). Thermal exposure from the fire is assumed to be characterised by a single temperature and a total heat transfer coefficient that is homogenised over the volume of a fire-resistance furnace. The fire resistance framework has been long criticised on the basis that both assumptions are very limited within their scope of applicability and do not adequately represent the temporal evolution of a fire in spaces consistent with contemporary architecture.

Recognising that further quantification of the fire environment was needed, a vast body of research conducted from the 1950s to the 1990s led to the development of the Compartment Fire Framework that quantifies the thermal boundary condition of real fires in small, cubic compartments with small openings where the fuel was fully involved in the fire (Torero *et al.* 2014). One of the critical outcomes from this work was the characterisation of the fire behaviour for "under-ventilated" compartment fires into a single temperature, which has enabled the study of the structural response to so-called "real fires" under very clear bounds of limitation (Torero *et al.* 2014).

The processes occurring in compartment fires traverse multiple length and timescales (Torero 2013); thus, simplifications to the description of the fire are required. In structural analysis, the conjugate coupling of the fire (gas-phase) and structure (solid-phase) is avoided by treating the fire as a thermal boundary condition to the solid-phase. This is possible because the gas and solid phase have very different characteristic thermal timescales (Torero 2013).

The structural response to the fire can be characterised by two behaviours: thermal expansion and thermal curvature, with the former associated with the average through depth temperature of the solid, and the latter associated with the thermal gradient in-depth within the solid (Usmani *et al.* 2001). Both the average temperature and the thermal gradient result from the solution to the energy conservation equation. Thus, the thermal boundary condition must be described as a rate of net convective and radiative heat transfer from the compartment fire imposed onto the structure, resulting in a total heat flux that defines the rate of heat transfer into the structure (Torero *et al.* 2017).

The existing Compartment Fire Framework (Torero *et al.* 2014) provided a solution to the thermal boundary condition; however, its application has been recognised as inconsistent with fire behaviour in larger (and more ventilated) open-plan compartments, which display significant heterogeneities in the thermal fields. Moreover, it was highlighted from the structural analysis of the Cardington Tests that the response of complex structural systems is particularly sensitive to the fire scenario, recommending the consideration of "post-flashover" and "spreading fires" in large compartments (The University of Edinburgh 2000). These gaps and outcomes from prior work have motivated further experimental work on characterising the fire dynamics of large open-plan compartment fires (Hidalgo *et al.* 2017). It was shown that the fire dynamics and thermal environment of open-plan compartment fires can be classified into three distinct modes of behaviour: a fully-developed fire, a growing fire, and a travelling (steadily moving) fire based on the ratio of flame spread velocity (V_S) and burnout front velocity (V_{BO}) (Hidalgo *et al.* 2019).

While numerous design methods have been developed to address specific fire modes independently, they all employ engineering level assumptions or models that have not been fully validated against experimental data consistent with this application, i.e. the large open-plan type compartment. A recent extensive review of the available fire models used to construct a thermal boundary condition for structural analysis has shown that these models target fully-developed or post-flashover fires in under-ventilated compartments or travelling fire models that employ a mobile localised plume approximation (Khan *et al.* 2021). In either case, no study has yet quantitatively extended the range of applicability of these models to open-plan compartments. This is owing to two key factors: (1) an insufficient knowledge of open-plan compartment fire dynamics, and (2) a lack of synthesis of the existing data and knowledge from large compartment fire experiments. Without an aggregated understanding of the current state-of-the-art in terms of open-plan compartment fire dynamics and any underpinning experiments, it is difficult to improve the existing models and identify the key features and details that should be incorporated and answered for future experiments. Consequently, it can be argued that a physical basis for the existing models does not yet exist.

This paper aims to address these two gaps by providing a review of the current state-of-the-art of open-plan compartment fire dynamics and by elucidating the nature of the thermal exposure imposed onto structural elements by these fires. This is achieved by compiling and analysing the experimental data collected from an exhaustive review of almost every open-plan type compartment fire experiment reported in the literature ($n = 37$), and considering the temporal and spatial distributions of all measured variables in the compartment. These experiments were conducted between 1993 and the present. The experiments were selected because they have the appropriate sensors to quantify the thermal boundary condition imposed on the ceiling. The spatial resolution of thermal exposure measurements varies amongst the experiments, with only a few having a sufficient resolution of sensors to characterise spatial heterogeneities. The experiments analysed are of a similar scale, however, the compartment configuration, fuel type, fuel load density, boundary conditions and ventilation vary considerably. This review paper focuses solely on quantifying the spatiotemporal distributions of fireimposed ceiling heat fluxes, thus, only the necessary details specific to each experiment are discussed. The overarching objective of this work is to synthesise the vast body of experimental work so as to elucidate the state-of-the-art knowledge on the behaviour and thermal exposure of real fires in large open-plan compartments. Gaps in the existing body of experimental research will be highlighted based on the results of the analysis to help steer future research. This paper intends not to supersede, but to complement existing reviews that have summarised the state-of-the-art modelling approaches and performance-based design methods used for quantifying the thermal exposure (Stern-Gottfried *et al.* 2010; Stern-Gottfried and Rein 2012; Torero *et al.* 2014; Dai *et al.* 2017; Khan *et al.* 2021).

2. Compartment Fire Dynamics and the Thermal Boundary Condition

The thermal environment within the compartment is defined by the interaction between the highly complex combustion processes occurring within the reaction zone front and the surrounding environment. Once a material is supplied with enough energy to raise the surface temperature to an ignition temperature, T_{ig}, ignition occurs, and a flame is established, thus initiating the fire event (Torero 2016). The feedback from the flame onto the fuel is used to initiate a series of ignitions leading to the process of flame spread (Fernandez-Pello and Hirano 1983), which is characterised by a flame spread rate, V_S. The flame will continue spreading if the characteristic time for ignition is smaller than the local burnout time of the fuel. This condition requires the burnout front velocity, V_{BO} to be approximately equal to or smaller than V_S and is dependent on the rate of fuel produced per unit area (local burning rate) and the mass of fuel (Drysdale 2011). Both V_S and V_{BO} define the surface area of combustible fuel participating in the fire.

In smaller compartments, the enclosing boundaries add further complexity as hot effluent gases and smoke released from the fire plume can accumulate locally within the upper regions of the compartment. These gases will transfer heat by convection and radiation to the boundaries of the compartment. Some fraction of heat from the smoke layer and compartment boundaries will radiate towards any combustible fuels in the lower regions of the compartment. If the geometry and thermal characteristics of the boundaries permit, sufficient irradiation onto the fuel will significantly enhance the rate of flame spread relative to the burnout front velocity ($V_S / V_{BO} > 1$). Once all the fuel is ignited, the compartment fills up with smoke and heats up very quickly as the heat feedback from the smoke layer and boundaries enhances the fuel burning rate, thereby introducing large quantities of energy, creating a feedback loop until the fire is "fully-developed" and the heat release rate (HRR) approximates a steady-state condition until burnout of the fuel. The transition to this steady-state region (where $V_S / V_{BO} \rightarrow \infty$) is referred to as flashover (Drysdale 2011). After flashover, the rate of fuel production exceeds the rate at which oxygen can be transported into the reaction zone through any openings within the compartment (windows, doorways etc.). Consequently, the compartment becomes oxygen-starved and the HRR is controlled by the rate of the oxygen supply through the openings. It was shown that under specific configurations (small compartment geometries with small openings), the compartment could be approximated as "well-stirred" with a homogenous thermal environment defined using a single temperature. Under these conditions, the oxygen supply to the reaction zone was directly related to the size of the opening, and thus all the parameters controlling the fire dynamics depend on the size of the compartment and openings leading to the definition of an inverse opening factor parameter ($\phi' = A_T/(A_0\sqrt{H_0})$). This characterisation of the compartment fire is referred to in the literature as "ventilation-controlled" or "*Regime I*" and has been extensively studied (Kawagoe 1958; Thomas and Heselden 1962; Gross and Robertson 1965; Thomas *et al.* 1967; Thomas and Heselden 1972; Harmathy 1972; Thomas 1973; Prahl and Emmons 1975), with a review of this work provided by Torero *et al.* (Torero *et al.* 2014). Based on the underlying assumptions of *Regime I*, numerous analytical methods to define either a gas temperature or heat flux thermal boundary condition for design purposes have been proposed (Law 1971; Thomas and Heselden 1972; Harmathy 1972; Law 1983; Law and O'Brien 1989). These methods were assimilated by the SFPE Task Group on Fire Exposure to Structures (SFPE, 2004) and used to develop the SFPE Engineering Standard on Calculating Fire Exposure (SFPE, 2011). It is important to emphasise that the independent

variable to calculating fire exposure in all these methods, despite their particularities, is the opening factor. A series of simple functions (f_1, f_2, f_3) have been shown to link the opening factor to the heat flux (Torero *et al*. 2014), thus

$$\langle \dot{q}''_{inc} \rangle \sim f_1(T_{g,\max}) \sim f_2(m_{O_2}) \sim f_3\left(\frac{A_T}{A_0\sqrt{H_0}}\right) \quad (1)$$

It was well recognised that the assumptions governing the behaviour of the *ventilation-controlled* regime (*Regime I*) no longer apply once the compartment geometry and openings are sufficiently large and the compartment becomes well ventilated. Thus, the thermal boundary condition is a conditional mean based on the compartment burning regime. Outside of the *ventilation-controlled regime*, products of combustion are expelled through the openings as fast as air is entrained into the fire (Torero *et al.* 2014). The result is a weaker hot gas layer that is not thermally stratified and with a short residence time. As a consequence, the flow field is controlled by the temperature gradient of the fire and the cold air surroundings, and therefore the pressure differentials generated by the fire dominate the entrainment rate into the fire, and the flow is momentum-driven. Under these conditions, the compartment fire dynamics and the thermal exposure cannot be explicitly defined by only $A_T/(A_0\sqrt{H_0})$. These fires are classically referred to as "fuel-controlled" or "*Regime II*" (Thomas *et al.* 1967; Thomas and Heselden 1972; Harmathy 1972). In this regime, a large scatter in the data was found, and the fire dynamics could not be linked to the size of the openings. It was believed that the high degree of scatter in the data was associated with complex transport processes controlling the burning behaviour of the fuel and the thermal environment inside the compartment. Subsequent experiments following the underpinning work from the Compartment Fire Framework with increased sensor resolution have demonstrated significant heterogeneities in the temperature fields both horizontally and vertically for compartments of similar geometries (Abecassis-Empis *et al.* 2008; Majdalani *et al.* 2016). Spatial distributions in the heat transfer from fully-developed fires in large compartments have been shown to elicit unique responses in the structural integrity of both single elements and systems (Jowsey 2006; Stern-Gottfried *et al.* 2010), particularly when compared to standardised time-temperature curves such as ISO 834 (International Organization for Standardization 1999) or the Eurocodes parametric fire curves (European Standard 1993).

Towards the scale of large open-plan compartments, heterogeneities in the temperature and heat flux fields increase dramatically for post-flashover fires (Welch *et al.* 2007; Stern-Gottfried *et al.* 2010; Gupta *et al.* 2021). Moreover, evidence collected from accidental fires and experiments have revealed that post-flashover conditions often do not occur in open-plan compartment fires as the compartment geometry and opening sizes of the compartment are sufficiently large such that smoke or hot gases cannot accumulate locally and sustain the necessary thermal feedback to the fuel to uniformly heat the compartment to a flashover condition (McCaffrey *et al.* 1981). Instead, the fire will spread through the compartment and burn over a finite area, with the burning area defined by the rate of spread of the flame front (V_S) and the burnout front (V_{BO}). The temperature heterogeneities introduced within these types of compartment fires are inevitably greater as a temperature gradient through the gas-phase is established from the region local to the fire (near-field), to the region remote from the fire (far-field). Given the finite burning area, total burnout of the fuel occurs much later than an ordinary fully-developed fire, in which the entire fuel load burns uniformly. Therefore, the duration of thermal exposure to the structure will far exceed those of typical design methods which are based on the *Regime I* characterisation.

Several engineering methods have been developed to approximate the heterogeneous thermal boundary condition that evolves in space and time for the case where the flame spread rate and burnout front rate are in equilibrium ($V_S/V_{BO} \approx 1$) over a fixed burning area, thus the flames move uniformly along the floor plate. These are referred to in the literature as travelling fires. Travelling fire methods in the literature can be demarcated into Clifton's model (Clifton 1996), Travelling Fires Methodology (TFM) and its subsequent iterations (Rein *et al.* 2007; Stern-Gottfried and Rein 2012; Rackauskaite *et al.* 2015; Heidari *et al.* 2019), and the Extended Travelling Fire Methodology (ETFM) (Dai *et al.* 2020). A review of some of these methods is presented by (Dai *et al.* 2017). Central to these methods is the definition of a near-field region and a far-field region that is defined by the burning area of the fire. The demarcation and treatment of the thermal exposure in the near-field and far-field were originally justified using the output of a computational fluid dynamics (CFD) calculation (Rein *et al.* 2007).

Later studies have substituted the CFD calculations with simple engineering correlations and/or assumptions to define the spatiotemporal evolution of the near-field and far-field regions (Stern-Gottfried and Rein 2012). These correlations and assumptions used in travelling fire models are derived from observations of maximum temperatures in small-scale compartment fire experiments and experiments investigating the interaction of impinging fire plumes and the flow of a ceiling jet along an unconfined ceiling (Alpert 1972; Alpert 1975; Pchelintsev *et al.* 1997; Wakamatsu *et al.* 2003). Ceiling jet and localised fire plume models are typically derived from gas burner experiments at various HRRs, meaning that the pyrolysis rate of the fuel (that drives the HRR) and thermal feedback processes are inherently decoupled. As a result, the HRR acts as the input for the model, which

defines the thermal boundary condition. In the context of compartment fires, these models have disconnected the thermal exposure from the fuel and compartment characteristics, and thus they are not related to V_S / V_{BO}. This is problematic in the sense that V_S / V_{BO} defines the burning area and thus the HRR (Gupta *et al.* 2021). Then, decoupling the fuel and compartment limits the applicability of the plume and ceiling jet correlations greatly. To circumvent these issues, the temporal evolution of the fire (spread rates) in travelling fire methods are predefined, and hence the methods are fixed to the condition where $V_S/V_{BO} \approx 1$. All that remains is to identify the appropriateness of the plume and ceiling jet correlations in delivering a boundary condition that is consistent with compartment fires for $V_S/V_{BO} \approx 1$. This is not well understood as the underpinning empirical correlations and simplifications applied in travelling fire methods do not consider interaction of the flow with the compartment boundaries. Subsequent iterations of the TFM have sought to refine the representation of the thermal fields, seeking to improve the approximation of the temperature gradient in the definition of the near and far-fields (Rackauskaite *et al.* 2015; Heidari *et al.* 2019). Nevertheless, while these improvements describe evolutions of localised fire models, they have still not been fully contrasted with appropriate large-scale compartment fire experimental data. Due to the uncertainty in the adequacy of the travelling fire submodels and the inherent restriction to $V_S/V_{BO} \approx 1$, a broad parametric sensitivity analysis is often required when applying travelling fire methods for design purposes.

Structural analyses that implement these methods have shown that the spatial temperature heterogeneities imposed onto a structure from travelling fires of smaller sizes induces unique and often more severe structural responses (Law *et al.* 2011; Stern-Gottfried and Rein 2012; Rackauskaite *et al.* 2017). However, in the absence of a benchmark to experimental data and an analysis of energy conservation within the compartment from the underlying methods, the degree of physical validity in the assumptions driving the models and the robustness of any structural analysis remains unquantifiable. Despite this, these methods have been widely adopted in fire safety engineering practice in the design of numerous tall buildings and have been recently incorporated into design standards.

Current simplified methods for travelling fires assume that the fire characteristics do not change as the fire spreads through the open-plan compartment. The extent to which this assumption remains valid has received little attention until very recently, although it has been observed qualitatively, as early as 1993, from the experiments conducted by the Building Research Establishment (BRE) at Cardington (Cooke 1998; Kirby *et al.* 1999) that fires in large compartments can spread in several modes. A concerted effort within the Real Fires for the Safe Design for Tall Buildings (RFSDTB) project has focused on elucidating the modes of fire spread and fire dynamics within large compartments through a series of large-scale experiments with the greatest instrumentation density within a compartment fire experiment to date. Three distinct modes of fire behaviour based on the ratio of the spread and burnout velocities (V_S / V_{BO}) were theorised based on observations from prior experiments:

- Mode 1: a fully-developed fire where $V_S / V_{BO} \rightarrow \infty$
- Mode 2: a growing fire where $V_S / V_{BO} > 1$
- Mode 3: a travelling fire where $V_S/V_{BO} \approx 1$

Each of the three distinct fire spread modes was subsequently identified during the evolution of the large-scale demonstrator Malveira Fire Test conducted within the RFSDTB project (Hidalgo *et al.* 2019). Examples of each mode from the test are shown in Figure 1. Flame spread and burnout front velocities, and therefore the time evolution of each mode was quantified.

Each fire spread mode was artificially simulated using controlled gas burners in the Edinburgh Tall Building Fire Tests (ETFT), which was a companion series of fire experiments in the RFSDTB project that were conducted in a separate large-scale compartment (Hidalgo *et al.* 2017). These experiments were designed to systematically control and characterise the thermal environment for each mode under varying ventilation conditions. The global energy balance of the compartment was calculated using the very large density of sensors in the experiments to obtain the distribution of energy losses from the fire source (Maluk



Figure 1. Observations of the fire spread modes during the Malveira Fire Test. (a) shows a travelling fire or Mode 3 ($V_S / V_{BO} \approx 1$) from 26 – 107 mins, (b) shows a growing fire or Mode 2 ($V_S / V_{BO} > 1$) from 107 - 237 mins, (c) shows a fully-developed fire or Mode 1 ($V_S / V_{BO} \rightarrow \infty$) from 237 - 241 mins at which point the fire was suppressed.

et al. 2017; Gupta *et al.* 2019; Gupta *et al.* 2021). Each fire spread mode was found to exhibit a characteristic spatial distribution of heat within the compartment. Nevertheless, the majority of the heat was lost by advection of the hot gasses through the openings irrespective of the fire spread mode and ventilation condition imposed resulting in an inability for a thermally stratified smoke layer to accumulate and descend within the compartment (Gupta *et al.* 2021). The thermal feedback from the smoke layer and compartment boundaries onto the fuel introduces a mechanism for enhancing the flame spread rate along the surface of the fuel in time. Consequently, it is possible to enhance V_S relative to V_{BO}, thus leading to the possibility for a transition from a travelling fire to either a growing fire (Mode 2) or fully-developed fire (Mode 1).

For porous fuel-beds such as wood cribs that are typically used in compartment fire experiments, V_{BO} can be regarded as a constant that is defined by the geometry and porosity of the wood crib (Gupta *et al.* 2021), however, for other fuels V_{BO} can be dependent on the quantity of fuel, and its total mass transfer number or B-number that defines the thermodynamic efficiency of burning of the fuel. Wood cribs are of particular interest as they are the dominant natural fuel used in most large-scale compartment fire experiments as the fuel loads are easy to quantify and they can sustain combustion without an external heat input. Recently, a detailed analysis of the burning processes in spreading wood crib fires in large compartments showed that wood crib approximates steady-state burning in a fuel-bed-controlled regime and a momentum-controlled regime (Gupta *et al.* 2021). In the fuel-bed-controlled regime, the fire corresponds to the travelling fire mode ($V_S/V_{BO}\approx 1$) as the porous crib is insulated from external effects from the compartment, thus the crib geometry controls the spread rates. Thermal feedback from the compartment and smoke layer onto the fuel was shown to be small in this regime. The momentum-controlled regime occurs when the fire is fully-developed ($V_S / V_{BO} \to \infty$), with very large heat fluxes external to the crib from the compartment and flame enhancing the fuel burning rate. The burning rate is controlled by complex inertia-driven flows and is heavily distributed spatially, with burning rates approximately 1.5 to 2 times larger than the fuel-bed-controlled regime due to strong radiative feedback, thus considerably more energy is introduced into the compartment in this regime. The independent variable controlling the burning regimes and fire spread modes is the thermal feedback onto the fuel-bed which enhances the spread rate over the surface of the wood crib. Therefore, transitions in the fire modes are driven by increases in the thermal feedback from the compartment to the fuel-bed surface, or by changing the ventilation conditions at the flame front which can strengthen the flame leading to sudden increases in the flame spread rate (Gupta *et al.* 2020).

Recent efforts aimed at characterising the fire dynamics of large open-plan compartments have shown that it is possible to define the evolution of real fires in terms of V_S / V_{BO}, a parameter that carries physical meaning (Gupta *et al.* 2020; Gupta *et al.* 2021). However, there have been limited attempts at quantifying the thermal boundary conditions of real fires. CFD models offer a pathway to resolving the spatial distribution of heating to the structure and have been used successfully a posteriori to treat the thermal boundary condition for very well-characterised compartment fire scenarios (Jowsey 2006; Jahn *et al.* 2011). However, the use of CFD to predict the evolution of V_S / V_{BO} a priori requires the resolution of very small length and timescales in the gas and solid phases that are inconsistent with the very large length scales associated with open-plan compartments typical of modern tall buildings. The computational cost to perform such a calculation at the detail needed to resolve complex flame spread and burnout processes would be prohibitive for any engineering-level calculation. Moreover, without an adequate understanding of the fire dynamics and fire-imposed heat fluxes in large open-plan compartments, the robustness of the various sub-models that underpin modern CFD codes cannot be verified and validated. This is due to a lack of large-scale experimental data that delivers an adequate spatial resolution consistent with field models and the level of repeatability required to enable the calculation of statistical moments to quantify the level of experimental uncertainty at the large scale (Torero 2013). By understanding the characteristics specific to each mode of V_S / V_{BO}, it could be possible to utilise CFD to model each mode without consideration of the fuel-compartment interaction, which would greatly simplify the issue of competing length and time scales. This would enable CFD to become a very useful tool to quantify the spatial and temporal distribution of the thermal boundary condition within a compartment that can serve as a coupled input to a thermomechanical model for a structure (Khan *et al.* 2021). Nevertheless, the experimental distribution of thermal exposure for each fire mode (V_S / V_{BO}) must be established to serve as a physical benchmark to steer CFD modelling approaches.

3. Experimental review

A first step to establishing an understanding of the thermal exposure in large open-plan compartments is to review and assimilate the available experiments and resulting data. The objective of this review will be to quantify the temporal and spatial distributions of thermal exposure that delivers the following thermal boundary condition to the opaque structure:

$$\dot{q}''_{net} = -k\frac{dT}{dx}\bigg|_{x=0} \tag{2}$$

where k is the thermal conductivity of the solid material

and $\dot{q}''_{net}$ is the net heat flux that is transferred into the structural element, thus it would generally be necessary to quantify the net radiative and convective exchange with the gas-phase. For this work, the thermal boundary condition is simplified to a total gauge heat flux defined as:

$$\dot{q}''_{inc} = \dot{q}''_{inc,rad} + h_c(T_g - T_0) \quad (3)$$

where $\dot{q}''_{inc,rad}$ is the incident radiant heat flux, measured from a radiative heat flux meter such as a radiometer, thin-skin calorimeter or plate thermometer. The convective component of the heat flux is defined by extracting T_g from the closest gas-phase temperature measurement to the heat flux meter and by setting T_0 as a cold reference temperature. It is important to note that this approach removes the need to quantify heat losses and decouples the definition of the thermal boundary condition from the heat diffusion equation. Further, this formulation provides a conservative estimation of the imposed convective heat flux. Using $\dot{q}''_{inc}$ as the external heat flux supplied to a boundary for the thermal analysis of a solid will always give conservative results.

The convective heat transfer coefficient is defined by assuming a forced flow over a horizontal plate (Bergman *et al.* 2011):

$$Nu = L_c h_c / k_{gas}(T) = 0.037 Re^{4/5} Pr^{1/3} \quad (4)$$

where the characteristic length L_c is assumed as 1 m and the Reynolds number (Re) is formulated by assuming a characteristic ceiling velocity (v_c) of 2.25 ms^{-1} based on statistical outputs from CFD analyses of large-scale compartment fires (Gupta *et al.* 2021). The assumptions are expected to only influence the results for $V_S/V_{BO} \approx 1$ and $V_S/V_{BO} > 1$, where the magnitude of irradiation inside the compartment is mild relative to a fully-developed fire (Gupta *et al.* 2021). It is worth noting that for forced convective flows as assumed here, the scaling dependency of the heat transfer coefficient h_c is weak for both the characteristic length: $h_c \sim L_c^{-1/5}$ and the characteristic velocity: $h_c \sim v_c^{4/5}$. Therefore, the approximation for these two terms is appropriate within the context of large compartment fire geometries. For certain sensors such as a water-cooled heat flux gauge or a steel billet, the total gauge heat flux $\dot{q}''_{inc}$ is directly obtained from the literature.

3.1. Experimental matrix

To perform this analysis, the spatiotemporal distributions in the heat flux boundary condition to the ceiling are extracted from 37 large-scale compartment fire experiments reported in the literature. The selected experiments comprise the majority of the large-scale experimental campaigns spanning from 1993 to 2019 and are compiled in Table 1. Some experiments are omitted from this analysis, notably the St. Lawrence Burns experiments (Shorter 1959; Gales 2014), the BRE Large Compartment Fire Test (Lennon 1998) due to the lack of reported fire characterisation. Furthermore, Cardington 7 is not included in this dataset as this was a reduced scale compartment. More recent experiments conducted at CESARE in Australia (Thomas *et al.* 2005) are also omitted as the compartment geometry was deemed to represent a corridor rather than an open-plan configuration.

The experiments selected for this analysis comprise varying geometries and ventilation configurations. The ratio V_S / V_{BO} is either controlled directly using gas burners and pool fires or is obtained as an outcome of a naturally spreading wood crib fire. As the fire development is either controlled by gas burners or is well characterised through experimental observations, the measured data in each experiment can be segmented by each mode of V_S / V_{BO} as a means of data reduction for each respective mode.

3.2. Data reduction and processing methodology

Various heat flux meters are used in the experiments, consisting of thin-skin calorimeters (Hidalgo *et al.* 2017), plate thermometers (Ingason and Wickström 2007; Häggkvist *et al.* 2013), steel billets (Masson 2003), radiometers and welded thermocouples on low-density metal sandwich panels (Hidalgo 2015). All these measurements (except for a radiometer) require a posteriori analysis to quantify the irradiation (incident radiant heat flux) or total gauge heat flux. The methodologies to calculate the heat flux from each type of sensor are provided in the respective references. Each experiment has a varying amount of heat flux meters; thus, a statistical analysis will be used to consolidate the spatial distribution of measured heat fluxes. A methodology for data reduction of the temporal distributions for each fire spread mode is proposed.

Recent experiments such as x-One/Two led by Imperial College London and the TRAFIR-Ulster campaigns led by Ulster University have not yet published heat flux data. The existing published data consists of a few near-ceiling thermocouples positioned along the length of the compartment. To assimilate the largest possible amount of data for this analysis, we have transformed the reported gas-phase temperatures to a total gauge heat flux for these experiments based on defining a characteristic total heat transfer coefficient specific to V_S / V_{BO}, which is obtained from the best representative experiments for each mode. Consequently, the gauge heat flux for x-One/Two and Ulster T1/T2 is estimated as

$$\dot{q}''_{\mathrm{inc}} = (h_{\mathrm{c}} + h_{\mathrm{r}}) T_{\mathrm{g}} = h_{\mathrm{T}} T_{\mathrm{g}} \quad (5)$$

where h_c is the convective heat transfer coefficient (calculated using equation (4)), h_r radiative heat transfer coefficient, and h_T is the total heat transfer coefficient that represents the summation of the convective and radiative heat losses. The total heat transfer coefficient has a functional relationship to the gas temperature and depends on the compartment fire conditions (which drives the convective

Table 1. Summary of experimental data obtained from the literature to be used for the analysis

Experiment ID	Reference	Year	Geometry (W × D × H)	ϕ' ($m^{-1/2}$)	Fuel	Sensor Qty	Observed modes (M1, M2, M3)[a]
Cardington 1	(Kirby *et al.* 1994)	1993	5.6 × 22.9 × 2.8	10.5	Wood crib	2	M2→ M1
Cardington 2	(Kirby *et al.* 1994)	1993	5.6 × 22.9 × 2.8	10.5	Wood crib	2	M2→ M1
Cardington 3	(Kirby *et al.* 1994)	1993	5.6 × 22.9 × 2.8	29.9	Wood crib	2	M2→ M1
Cardington 4	(Kirby *et al.* 1994)	1993	5.6 × 22.9 × 2.8	29.9	Wood crib	2	M2→ M1
Cardington 5	(Kirby *et al.* 1994)	1993	5.6 × 22.9 × 2.8	57.7	Wood crib	2	M2→ M1
Cardington 6	(Kirby *et al.* 1994)	1993	5.6 × 22.9 × 2.8	236.7	Wood crib	2	M2→ M1
Cardington 8	(Kirby *et al.* 1994)	1993	5.6 × 22.9 × 2.7	11.5	Wood crib	2	M2→ M1
Cardington 9	(Kirby *et al.* 1994)	1993	5.6 × 22.9 × 2.8	11.4	Wood crib	2	M1
ECSC 1	(Lennon and Moore 2003)	1999	12 × 12 × 3.4	10	Wood crib	1	M1
ECSC 2	(Lennon and Moore 2003)	1999	12 × 12 × 3.4	10	Wood Crib	1	M1
ECSC 3	(Lennon and Moore 2003)	1999	12 × 12 × 3.4	10	Wood Crib	1	M1
ECSC 4	(Lennon and Moore 2003)	1999	12 × 12 × 3.4	14.3	Wood crib	1	M1
ECSC 7	(Lennon and Moore 2003)	2000	12 × 12 × 3.4	14.3	Wood crib	1	M1
ECSC 8	(Lennon and Moore 2003)	2000	12 × 12 × 3.4	10	Wood crib	1	M1
Vaseli	(Horová *et al.* 2013)	2011	12 × 9 × 4	18	Wood crib	5	M2→ M1
ETFT 1	(Hidalgo *et al.* 2017)	2013	17.8 × 4.9 × 2	4.1	Propane gas	45	M1
ETFT 2	(Hidalgo *et al.* 2017)	2013	17.8 × 4.9 × 2	4.1	Propane gas	45	M2
ETFT 3	(Hidalgo *et al.* 2017)	2013	17.8 × 4.9 × 2	4.1	Propane gas	45	M3
ETFT 4	(Hidalgo *et al.* 2017)	2013	17.8 × 4.9 × 2	23.3	Propane gas	45	M1
ETFT 5	(Hidalgo *et al.* 2017)	2013	17.8 × 4.9 × 2	23.3	Propane gas	45	M2
ETFT 6	(Hidalgo *et al.* 2017)	2013	17.8 × 4.9 × 2	23.3	Propane gas	45	M3
ETFT 7	(Hidalgo *et al.* 2017)	2013	17.8 × 4.9 × 2	4.1→23.3	Propane gas	45	M1
ETFT 8	(Hidalgo *et al.* 2017)	2013	17.8 × 4.9 × 2	4.1→23.3	Propane gas	45	M1
ETFT 11	(Gupta *et al.* 2020)	2013	17.8 × 4.9 × 2	4.1	Wood crib	45	M2 → M1
ETFT 12	(Gupta *et al.* 2020)	2013	17.8 × 4.9 × 2	23.3	Wood crib	45	M2 → M1
Malveira	(Hidalgo *et al.* 2019)	2014	21 × 4.7 × 2.85	4.6	Wood crib	24	M3 → M2→ M1
Tisova	(Rush *et al.* 2020)	2015	18 × 11 × 4.7	8	Wood crib	24	M3 → M2→ M1
x-One	(Heidari *et al.* 2020)	2017	35.5 × 10.8 × 3.2	16.1	Wood crib	3	M2 → M1
GFT PF2	(Sjostrom *et al.* 2019)	2018	18 × 6 × 3	1.8	Diesel pool	17	M3
GFT PF3	(Sjostrom *et al.* 2019)	2018	18 × 6 × 3	1.8	Diesel pool	17	M3
GFT PF4	(Sjostrom *et al.* 2019)	2018	18 × 6 × 3	1.8	Diesel pool	17	M3
GFT PF5	(Sjostrom *et al.* 2019)	2018	18 × 6 × 3	2.6	Diesel pool	17	M3
GFT WC	(Gupta *et al.* 2020)	2018	18 × 6 × 3	2.3	Wood crib	17	M3
x-Two.1	(Heidari *et al.* 2020)	2019	35.5 × 10.8 × 3.2	16.1	Wood crib	3	M3 → M2→ M1
x-Two.2	(Heidari *et al.* 2020)	2019	35.5 × 10.8 × 3.2	16.1	Wood crib	3*	M3
Ulster T1	(Nadjai *et al.* 2020)	2019	15 × 9 × 2.9	1.3	Wood crib	5*	M3
Ulster T2	(Charlier *et al.* 2020)	2019	15 × 9 × 2.9	3.3	Wood crib	4*	M3

* No heat flux meters, heat fluxes are inferred using gas-phase temperature measurements and a fitted global heat transfer coefficient (h_T)
[a]M1, M2, and M3 refer to Mode 1 ($V_S / V_{BO} \to \infty$), Mode 2 ($V_S / V_{BO} > 1$), and Mode 3 ($V_S / V_{BO} \approx 1$) respectively. The observed transitions from one mode to another are denoted by the arrow. e.g. M2→M1 refers to an experiment that comprises of two modes with a transition from Mode 2 to Mode 1.

and radiative losses). It would be expected that this quantity varies as a function of V_S / V_{BO} due to the dependence of this parameter on the fluid mechanics and heat and mass transfer mechanisms specific to each mode (Gupta *et al.* 2021; Gupta *et al.* 2021). As there is considerable spatial heterogeneity in these experiments,

the location of the thermocouple in relation to the fire location will be expected to influence h_T, therefore it is necessary to demarcate a characteristic near-field and far-field quantity for the proceeding analysis.

An empirical formulation of h_T can be extracted from experimental data with conditions that closely align with the experiments that this work seeks to transform from gas temperatures to heat fluxes (x-One/Two and Ulster T1/T2). These experiments consist of a wood crib fuel-bed under well-ventilated conditions. For $V_S/V_{BO}\approx 1$, which is steady-state, a value of h_T will be calculated for both the near-field and far-field using the heat flux and local gas temperature data measured from the GFT WC experiment. This calculation is based on equation (4). This experiment is well-characterised and exemplifies the travelling fire mode ($V_S/V_{BO}\approx 1$) (Sjostrom *et al.* 2019; Gupta *et al.* 2020), with flames also impinging on the ceiling, thus a larger (and more conservative) value for h_T is expected. Under increasing heat transfer conditions when the fire is growing ($V_S/V_{BO}>1$), h_T must be approximated in terms of the gas temperature T_g. If heat transfer within the compartment fire is not yet dominated by radiation, this dependence can be approximated by a linear fit with the convective heat transfer coefficient set as the y-intercept assuming that convective losses are dominant. This is a reasonable approximation for all regimes except the fully-developed condition ($V_S/V_{BO}\rightarrow\infty$), where radiation heat transfer is dominant due to the very large temperatures and optically-thick nature of the flames and smoke layer (Gupta *et al.* 2021). Similar approximations have been used to obtain h_T empirically for the ignition of solids (Hidalgo 2015). The exemplar experiments selected for empirically fitting h_T for $V_S/V_{BO}>1$ are ETFT 11, ETFT 12 and Malveira. In these experiments, $V_S/V_{BO}>1$ is clearly defined, with the spread and burnout rates quantified (Gupta *et al.* 2020). Moreover, these experiments have numerous sensors, which can be used to construct a statistical distribution of the fitting parameters for h_T, while considering their spatial variations. In the same approach, h_T is calculated at each spatial measurement point based on local measurements of the gauge heat flux ($\dot{q}''_{inc}$), the median value of the calculated h_T for $V_S/V_{BO}\approx 1$ and the slope of the fitted curve ($V_S/V_{BO}>1$) from all the sensors. The two modes are presented in Table 2.

Empirical approximations of h_T do not work when $V_S/V_{BO}\rightarrow\infty$ as radiation is the dominant heat transfer mode and the flow conditions are highly complex (Gupta *et al.* 2021). Approximating this term requires significant assumptions of the optical environment within the gas-phase. Such an approximation was undertaken by Jowsey (Jowsey 2006) for a fully-developed compartment fire, who showed that for an optically-thick medium at 1200ºC, $h_T\approx 207$ W/m^{2}K. This value for h_T was shown to be consistent with an analysis of the thermal fields and optical properties in a fully-developed compartment fire experiment (ECSC 8) (Welch *et al.* 2007). The value for h_T defined for fully-developed fires is significantly larger than those extracted from the experiments for both Mode 2 ($V_S/V_{BO}>1$) and Mode 3 ($V_S/V_{BO}\approx 1$) in Table 2. The disparity in h_T for both the travelling and spreading fires relative to Jowsey's canonical example for a fully-developed fire hints at the fundamental differences in the fire dynamics and heat transfer mechanisms defining the thermal exposure across the modes. Due to the challenges highlighted earlier, this work does not attempt to approximate the heat transfer coefficient for $V_S/V_{BO}\rightarrow\infty$. Further experimental research focusing on the physical characterisation of *Regime II* fire dynamics that satisfy the condition of $V_S/V_{BO}\rightarrow\infty$ are required to elucidate the dominant heat transfer mechanisms. This paper will simply present the reduced data for each mode to show that the heat transfer mechanisms and thermal exposures are distinct.

Table 2. Summary of total heat transfer coefficients used to transform gas-phase temperatures to total gauge heat fluxes through equation (5) for the x-One, x-Two.1, x-Two.2, Ulster T1 and Ulster T2 experiments

Fire Spread Mode (Dimensionless)	Total heat transfer coefficient (h_T) (W/m^2 K)
$V_S/V_{BO}\approx 1$	Near-field: 30.9 Far-field: 17.6
$V_S/V_{BO}>1$	$h_T = 0.031T_g + 11.3$

The total gauge heat flux for the remaining experiments reporting incident radiative heat flux measurements ($\dot{q}''_{inc,rad}$) are calculated from equation (3). The convective heat flux component (assuming a cold reference surface) is calculated for each measurement from equation (4) following the procedure detailed in Section 3. An analysis of the convective heat transfer coefficient calculated using equation (4) for a range of the experimental data yields a median value of $h_c = 11.27$ W/m^2 K. Due to the large characteristic length-scales of the boundaries in the experimental compartments (flat plate ceilings), the quantification of convective heat transfer coefficient is conservative, particularly considering that impingement of the plume on the ceiling is a stagnation point and that any ceiling jet formation away from the opening is dampened by stratification of the smoke layer.

The proceeding sections detail the data reduction approach corresponding to each of the identified fire spread modes that have been applied to each of the experimental data sets.

3.2.1. Mode 1: Fully-developed fire mode ($V_S/V_{BO}\rightarrow\infty$)

The quasi-steady assumption is employed for this mode ($V_S/V_{BO}\rightarrow\infty$) based on previous analyses of the compartment fire dynamics (Gupta *et al.* 2021). Therefore, the temporal evolution of the heat flux in this mode can be reduced by obtaining the mean heat flux for each

sensor over a time period. Signals for each sensor are averaged, where practicable, for the entire period of the fully-developed mode ($V_S / V_{BO} \rightarrow \infty$). If the wood crib fuel is ignited simultaneously, such as in the ECSC tests, the data is sampled for the period where the normalised mass loss of the crib ranges within 80% and 30% of the original mass following the approach by Thomas and Heselden (Thomas and Heselden 1972). For experiments where the fuel is not simultaneously ignited and the fully-developed mode arises as a natural outcome of fire propagation, the period upon transition to $V_S / V_{BO} \rightarrow \infty$ until burnout or suppression is taken as the averaging window. For specific wood crib experiments (ETFT 11 and ETFT 12), the fire is suppressed once rapid flame spread occurs over the top surface of the crib (but not in-depth within the crib), therefore the fire is not truly fully-developed. In these cases, the data is taken just before suppression as a reference, but this data does not capture the entirety of the burning crib. Thermocouple temperatures are not transformed to heat fluxes for this mode as the spatial resolution of the optical properties of the gas-phase is required (Welch *et al.* 2007), which are not available from any of the published experiments.

3.2.2. Mode 2: Growing fire mode ($V_S / V_{BO} > 1$)

This mode characterises the transition from a travelling fire to a fully-developed fire and is therefore transient in nature. Consequently, the complete temporal evolution of the heat flux for each sensor must be considered in the analysis. It would be expected that the heat flux evolution monotonically increases as the fire grows (except for controlled gas burners) due to the positive feedback loop leading to the continually increased heating within the compartment, and therefore a continually increasing flame spread rate. Based on measured flame spread rate data reported from experiments satisfying the condition $V_S/V_{BO}>1$ (Gupta *et al.* 2020), the flame spread rate evolution in time appears to follow an exponential growth behaviour. A generalised exponential function in the form $\dot{q}''_{inc}(t) = A\exp(kt)$ is fit to each of heat flux measurement point for the experiments within Mode 2 ($V_S/V_{BO} > \infty$). The fitting procedure consists of utilising a non-linear least squares approach to optimise the pre-exponential constant (A) and the growth rate constant (k). This approximation was found to be appropriate for most of the experiments, with the coefficient of determination (R^2) generally exceeding 0.90. The only exceptions were for ETFT 2 and ETFT 5, which are gas burner experiments where the spread rate is controlled and independent from the thermal conditions within the compartment. Nevertheless, those experiments are still fit to the curve for the comparison. The growth rate constant, k, which is a constant of proportionality delivering the time derivative of the heat flux is used to benchmark the heat flux growth rates across each experiment. This is physically significant, as a larger value for k indicates more significant (and faster) heating within the compartment, and is a useful surrogate for the evolution of the flame spread rate, which would be expected to follow the heating rate.

3.2.3. Mode 3: Travelling fire mode ($V_S / V_{BO} \approx 1$)

Assuming that a travelling fire behaves as a localised fire that propagates inside a compartment, an approximation of a near-field and far-field zone (Stern-Gottfried and Rein 2012), can be used to demarcate the temporal evolution of the measured heat flux at each sensor location inside the compartment. Moreover, it is assumed that the travelling fire approximates quasi-steady heating conditions in both the near-field and far-field regions. This effectively reduces the temporal evolution of the heat flux within Mode 3 ($V_S/V_{BO}\approx 1$) to a mean heat flux for the near-field and the far-field region at each measurement point in the experiments. Therefore, the spatial distri-bution of the mean near-field and far-field heat fluxes can be quantified within the compartment. The demarcation point of the near-field and far-field regions at each sensor is determined using a multiple changepoint detection algorithm that identifies an abrupt statistical (mean and RMS) change in the magnitude of the output for each heat flux signal. The abrupt change in signal and the magnitude of the signal defines the transition from the far-field to near-field or vice-versa. The mean of the signal is taken over the period for the near-field or far-field signal and defines the mean heat flux. Near-field heat fluxes correspond to the maxima of the signal output, while far-field heat fluxes are the minima. Details of the algorithm are provided elsewhere (Killick *et al.* 2012), and it has been programmatically incorporated into MATLAB.

Some complications arise for the experiments using diesel pool fires (GFT) which have controlled ignition times and where the fuel source only spans half the compartment length leading to signals that exhibit numerous peaks and troughs. In this case, a "peakfinder" algorithm is used along with a threshold of 10 kW/m^2 to delineate the near-field and far-field time windows within the signal. The signal is then averaged between the signal peaks to identify a mean near-field heat flux. The signal outside of this region is denoted as the far-field, and the mean of all the values is taken to extract the far-field heat flux. Further details on the implementation of these algorithms in the data processing of the travelling fire experiments (Mode 3) are provided elsewhere (Gupta 2021).

4. Results & Discussion

4.1. Fully-developed fire experiments

The spatial and temporal distribution of mean total gauge heat fluxes for the steady-state fire spread modes ($V_S/V_{BO}\approx 1$ and $V_S/V_{BO}\rightarrow\infty$) are calculated for each experiment from Table 1. Each mode is presented as a box plot to highlight the distribution of heat fluxes for each experiment. The data points on each plot indicate

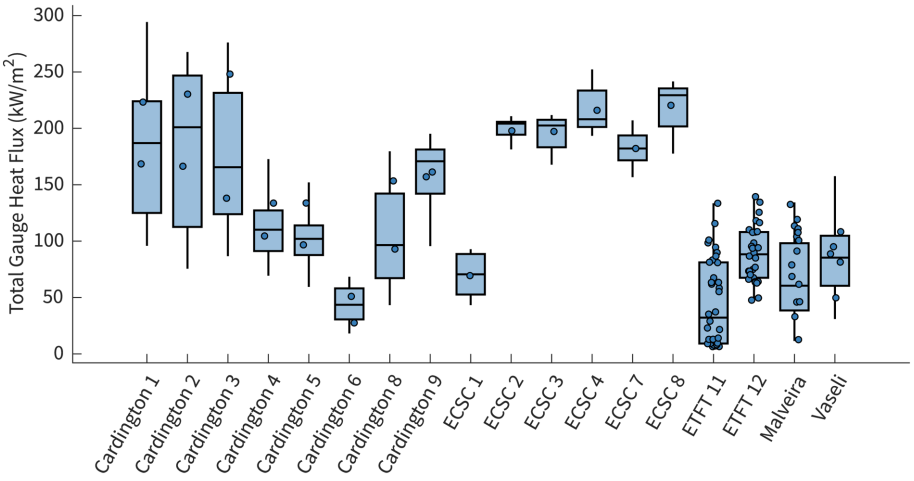


Figure 2. Box plot comparison of the estimated total gauge heat flux for each fully-developed compartment fire ($V_S / V_{BO} \rightarrow \infty$) experiments consisting of wood crib fuels from the literature. The range in each box plot shows the spatial and temporal distribution of heat fluxes.

the mean heat flux for each sensor that comprises the ensemble of temporal data. The more data points present indicates a higher instrument density (i.e. more measurement points spatially). The data points within each box are jittered to provide clarity to the plot. Figure 2 shows the distribution of the experimental data for the fully-developed fire spread mode ($V_S / V_{BO} \rightarrow \infty$ / Mode 1) with solely wood cribs.

Only the results for the wood crib experiments are presented within this section as the gas burner experiments from the ETFT experimental campaign, which imposes $V_S / V_{BO} \rightarrow \infty$, exhibits a unique behaviour that is associated to the low input HRR. This characteristic helps elucidate some characteristics of the travelling fire experiments and the data will be shown in the proceeding section.

The results from Figure 2 show a very large distribution of heat fluxes for $V_S / V_{BO} \rightarrow \infty$ across the different experimental data assimilated from the literature. Measured heat fluxes are directly related to the heat release rate (HRR) of the fire source in the compartment, with reported HRRs ranging within 25 MW - 45 MW for experiments such as those in the ECSC series. In these cases, mean heat fluxes can exceed 200 kW/m^2, peaking approximately 250 kW/m^2 for Cardington 3. The Cardington experiments are particularly unique as the compartment geometry was fully enclosed except for a single opening at one end, measuring approximately 23 m deep, thereby forming a corridor-like shape. This configuration varies considerably from the other experiments, which are not very deep. Each experiment except for Cardington 9 was ignited at the rear wall and allowed to propagate freely towards the opening. Large heat fluxes are immediately measured at the back of the compartment upon ignition, which rapidly decays once the flames spread along the surfaces of each wood crib towards the opening. The decay in the back wall is associated with the blockage of heat resulting from the descending smoke layer. Concurrently, heat fluxes peak at the opening as the oxygen concentrations are considerably larger due to the entrained air leading to downward spread and involvement of the wood crib in the burning process. A unique phenomenon occurs as the heat fluxes at the rear-wall start increasing dramatically as the wood cribs towards the opening burn out and the cribs start burning backwards as the smoke layer rises and oxygen can be further entrained deeper into the compartment. Cardington 9, which is uniformly ignited, impose relatively uniform heat fluxes in both the front and rear of the compartment.

Homogeneity in the thermal fields is not observed in the remainder of the experiments. While there is only a single heat flux meter present in the ECSC (Cardington NFSC2) tests, radiation fields generated by gas-phase temperatures of these experiments by Welch *et al.* (Welch *et al.* 2007) show significant radiative heat flux gradients across the ceiling plane. For experiments with a significant quantity of heat flux meters such as the ETFT series, Malveira Fire Test and the Vaseli Fire Test, the measured heat fluxes across the ceiling are highly heterogeneous. Contrasting the spatiotemporal distributions of the heat fluxes from the Cardington experiments with the other experiments highlights the importance of the compartment configuration and the fire evolution in defining the degree of heterogeneity.

The magnitude of measured heat fluxes from the wood crib experiments is comparable (and are often larger) than smaller-scale compartment fire experiments using realistic fuels that fit (theoretically) within the framework of *Regime I* (Jowsey *et al.* 2007). It is worth noting that the experiments presented herein for the fully-developed fire mode span the range of possible opening factor extremes. This is shown in Figure 3, which compares the peak total

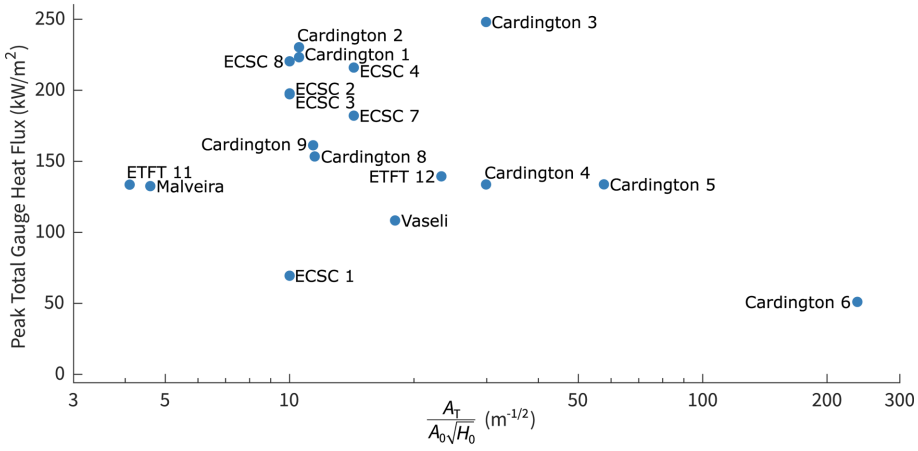


Figure 3. Peak total gauge heat flux for each fully-developed compartment fire ($V_S / V_{BO} \rightarrow \infty$) experiment with wood cribs presented as a function of the inverse opening factor (ϕ').

gauge heat flux from each experiment with the classical inverse opening factor. This plot is analogous to Thomas and Heselden's plot, which compares the maximum gas temperature to the inverse opening factor, showing a demarcation of the fully-developed compartment fire regimes to the theory.

The complexity in defining the thermal conditions of large compartment fires is exemplified by the large scatter in the data in Figure 3. The experiments with the largest heat fluxes are generally centred around $\phi' \approx 10$ m$^{-0.5}$. This outcome mirrors the classic CIB experiments (Thomas and Heselden 1972), which were conducted at a smaller scale, however, the scatter is still too significant to draw any conclusions. The only definitive conclusion that can be drawn from the data is the comparably smaller heat fluxes once the openings are reduced substantially ($\phi' \rightarrow \infty$), indicating that the oxygen concentration very much plays a role in determining the compartment temperatures at significantly small opening sizes, much like the classical theory (Thomas and Heselden 1972; Torero *et al.* 2014). Nevertheless, from the general trend and scatter from the data, it is clear that the thermal exposure cannot be correlated to the opening factor, even though some experiments with limited openings (ETFT 12 and Vaseli) would be theoretically classified into *Regime I* based on just the opening factor criterion defined by the outcomes of the CIB experiments (Drysdale 2011). One distinction may be the Cardington experiments, which based on qualitative and quantitative observations (Cooke 1998), are consistent with the description of *Regime I*, where generally, the heat flux decreases at larger opening factors.

An interesting point of comparison is the ECSC 1 and ECSC 8 experiments, which are identical in terms of the opening factor, fuel type and fuel load density except for an insulative spray that is applied on the ceiling for ECSC 8. This change reduces the thermal inertia of the ceiling material and leads to significantly larger measured heat fluxes as the solid phase reaches thermal equilibrium with the gas phase faster. Consequently, the heat losses from conduction through the ceiling linings are reduced substantially.

Fuel load density is an important parameter that was identified for small fully-developed compartment fire experiments, as an increased fuel load density results in a larger mean temperature as thermal equilibrium is attained faster. It is difficult to ascertain the importance of this parameter at larger scales. The fuel load densities within the Cardington experiments vary within 20 kg/m^2 and 40 kg/m^2 (Cardington 1 and Cardington 4), the ECSC tests are constant at 40 kg/m^2, the ETFT experiments are approximately 29 kg/m^2, the Malveira Test is 23 kg/m^2, and the Vaseli Fire Test is approximately 10 kg/m^2. It appears that there is insufficient variability in the fuel load densities across the reported experimental data to draw any statistical conclusions. A follow-up multiple regression analysis was undertaken on the mean heat flux data and several explanatory variables such as the inverse opening factor, fuel load density, compartment geometry, and thermal inertia of the ceiling lining materials (Gupta 2021). It was demonstrated that the existing variability in the experimental data for these variables is insufficient to draw any conclusions on the controlling parameters for the dynamics and thermal exposure from fully-developed compartment fires in large open-plan type compartments.

These results serve as a reminder of the complex interplay of parameters that ultimately defines the heat fluxes imposed onto the structure for a fully-developed large open-plan compartment fire. This is particularly emphasised for compartments with larger opening areas, which show a significant scatter in the data. The majority of the large compartment fires analysed in this study exhibit behaviour that show sufficient heterogeneities or have sufficiently large openings such that they tend towards the conception of Thomas' *Regime II* or the fuel-controlled compartment fire. Noting that the two fully-

developed regimes represent liming conditions in a compartment (Majdalani *et al.* 2016), it is very likely that many of these experiments may exhibit characteristics of both regimes. This was found to be the case for considerably smaller compartments. Well-stirred and hydrostatic conditions cognisant of *Regime I* were only attained for very large inverse opening factors: $\phi' \approx 70.1$ $m^{-0.5}$, which is consistent, at least qualitatively, with the Cardington test data from Figure 3. Nevertheless, there is not enough experimental data on key parameters such as the internal flow fields to quantitively explore this.

These types of fires are not physically understood, and the available data remains insufficient to elucidate the fire dynamics; thus, a model cannot be postulated to predict thermal exposure. However, these results challenge the notion that under-ventilated cubical (*Regime I*) compartment fires, or even large compartments with small openings impose "more severe" thermal conditions on the structure than a well-ventilated compartment more consistent with the original definition of *Regime II*. The magnitude of the heat fluxes found within the available experimental data are consistent with the classical CIB experiments, however, the exception in this case, is the significant spatial heterogeneities in heating that are manifested in the intricate coupling of the complex flow transport processes with the fuel. Existing design frameworks dependent on an opening factor to define fully-developed compartment fire behaviour such as the Eurocodes parametric fires or the Compartment Fire Framework clearly fall outside the bounds of applicability for large open-plan type compartment fires. Alternative approaches which explicitly address the significant uncertainty associated with this mode are required to define an appropriate thermal boundary condition for structural analyses.

4.2. Travelling fire experiments

The spatial distribution of the mean total gauge heat fluxes from the 13 travelling fire experiments ($V_S / V_{BO} \approx 1$) are calculated and demarcated by the near-field and far-field regions following Section 3.2.3 and the results are shown in Figure 4. The data from the experiments is also demarcated by the fuel type used, which consisted of wood cribs, diesel pools, and propane gas burners. The shaded bars correspond to the experiments where the heat fluxes were obtained by transforming near-ceiling gas temperature measurements through the empirical total heat transfer coefficients (h_T) defined in Table 2.

Contrasting the measured heat fluxes of the near-field and far-field for the travelling fire experiments ($V_S / V_{BO} \approx 1$) shows that the magnitude of heat fluxes is of an order of magnitude smaller than the experimental data for the fully-developed fire mode ($V_S / V_{BO} \to \infty$). Peak mean heat fluxes for the near and far-field regions rarely exceed 25 kW/m^2 and 12 kW/m^{2,} respectively. In a similar manner to $V_S / V_{BO} \to \infty$, there are significant spatial variations in the heat flux for each compartment. However, in absolute terms, this difference is not significant due to the small magnitude of heat fluxes. In both regions, the largest heat fluxes are found for the experiments consisting of diesel pool fires. This result is not surprising as diesel has a large mass transfer number and burns incompletely, thereby releasing large mass fractions of soot. The sooting nature of diesel enables the development of an opaque smoke layer that stratifies over the ceiling with a large radiative fraction. Considerably less opaque smoke layers form in the wood crib and gas burner experiments, thus heat is delivered to the ceiling primarily by convection from the fire plume. It is quite

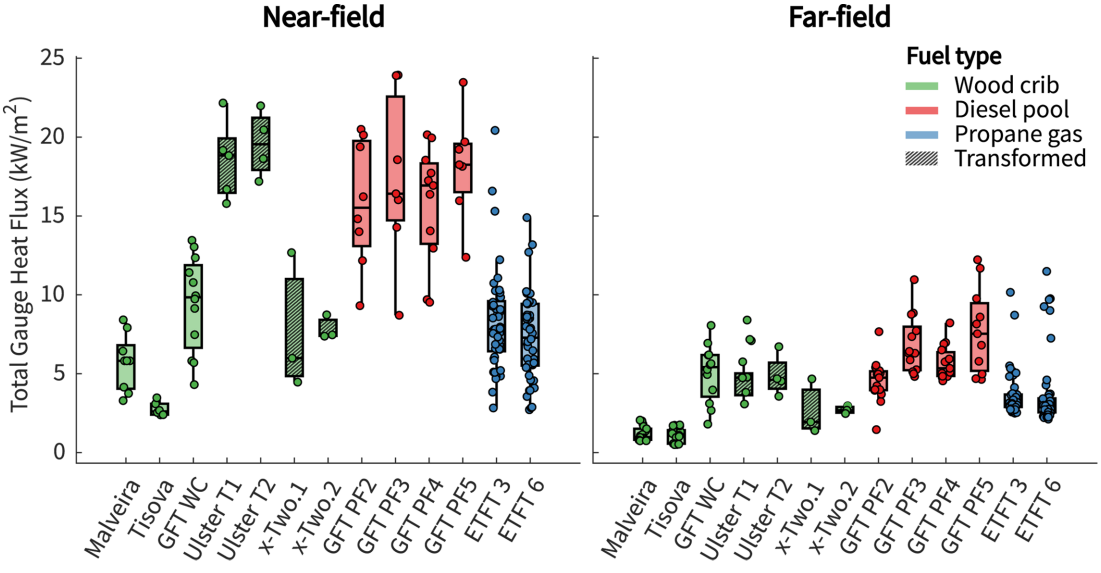


Figure 4. Total gauge heat fluxes in the near-field and far-field for each travelling fire experiment ($V_S / V_{BO} \approx 1$).

interesting to note the large heat fluxes for the Ulster T1 and Ulster T2 experiments, which use wood cribs, albeit in a rather unique configuration (rotated 60° from layer-to-layer) based on recent experimental work (Gamba *et al.* 2020) in an attempt to induce radial fire spread. This has the effect of promoting larger flame heights when compared to typical line fires from the other experiments leading to larger convective heat fluxes imposed onto the ceiling. Observations from field-scale experiments with cribs and other porous fuel-beds have shown that line fires of a similar nature to the experiments from this study are subject to flow instabilities causing localised flame peaks and troughs over the width of the fire and a "saw-tooth" flame geometry (Finney *et al.* 2015). Consequently, flame heights are not solely determined by the total burning area of the crib (exposed wood area). Nevertheless, an absence in the formation of an optically thick smoke layer for this experiment and all of those except for the diesel pool fires leads to smaller far-field heat fluxes.

The results presented herein for the travelling fire experiments are a considerable departure from existing performance-based design methodologies suggesting that the near-field is characterised by continuous flame impingement such as the Travelling Fires Methodology (Stern-Gottfried and Rein 2012). This assumption leads to very large and over-dimensioned heat fluxes in the near-field, with a far-field that monotonically decreases with a significant gradient due to "ceiling-jet" type flows along the ceiling. The evidence from all the data collected from travelling fire experiments suggests that these approximations of the open-plan compartment fire dynamics are significantly over conservative and the thermal exposure from travelling fires is minor. As the thermal feedback effect onto the fuel is limited in this regime, direct and continuous flame impingement and extension along the ceiling is unlikely as the burning rates are not enhanced. If one was to employ methodologies such as the TFM (and its subsequent iterations) or the ETFM, which both make approximations of continuous flame impingement, the imposed ceiling heat fluxes obtained from these methods are more consistent with fully-developed fire experiments (exceeding 100 kW/m^2) (Heidari *et al.* 2019; Dai *et al.* 2020). Such magnitudes can only be attained by introducing a considerable amount of energy into the compartment, which almost certainly, would induce very large quantities of thermal feedback due to a rapidly developing smoke layer. This would quickly raise the surface temperature of the fuel and transition the fire from "travelling" (Mode 3) to fully-developed (Mode 1) in a short period. The small heat fluxes from Figure 4 indicate that the heating imposed onto the ceiling for a travelling fire ($V_S/V_{BO} \approx 1$) is primarily controlled by convective heating from the fire plume (without continuous flame impingement). Convective heating is supplemented by mild irradiation from the flame and resultant ceiling jet that is not particularly hot and optically thick. These heat transfer mechanisms diverge considerably from the approximations underpinning the existing state-of-the-art travelling fire methods, and thus should be revisited in light of this data.

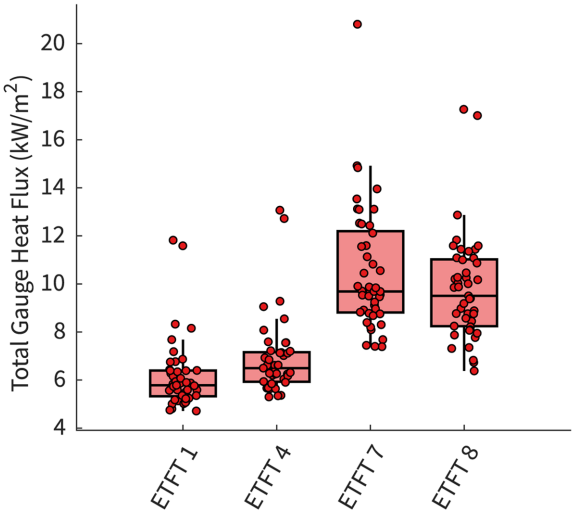


Figure 5. Total gauge heat fluxes for the Edinburgh Tall Building Fire Tests (ETFT) gas burner experiments that simulate a fully-developed fire mode ($V_S / V_{BO} \to \infty$).

Another aspect worth discussing is the fire size, which in the experiments presented thus far, are relatively small (ranging from 0.5 m to 3.5 m in length) compared to the floor plate length. The effect of the fire size at the relatively small HRRs (2.5 MW) are examined through the results of the gas burner experiments from the ETFT campaign that artificially simulate $V_S/V_{BO} \to \infty$ (Mode 1). The distributions for each gas burner experiment are shown in Figure 5.

The ETFT gas burner experiments intend to simulate $V_S/V_{BO} \to \infty$ through 12x propane gas burners (0.5 m × 0.5 m) distributed over the entire compartment floor plate (Hidalgo *et al.* 2017). The magnitude of the heat fluxes from these experiments, shown in Figure 5, are small and consistent with the travelling fire experiments from Figure 4. These results indicate that the imposed heat fluxes result from similar heat transfer mechanisms that define the near-field from the travelling fire experiments ($V_S/V_{BO} \approx 1$), which is that heating is primarily controlled by convective heating from the fire plume. This is further reinforced given the low sooting nature of propane gas. The differences in the values across the experiments are associated with changes in the ventilation conditions, with ETFT 1 and ETFT 4 being very well-ventilated and under-ventilated with static opening conditions and dynamic ventilation conditions in ETFT 7 and ETFT 8 (Hidalgo *et al.* 2017). The imposed ventilation condition has the effect of modifying the plume dynamics, and therefore the local heating to the plume (Gupta *et al.* 2021), however, the overall effect of these changes is small. Outside of the plume region, the inertia in the flow

is weak and the hot gas layer is thermally stratified. Thus, these fires exhibit drastically different behaviour when compared to fully-developed fires involving wood cribs. Instead, these experiments behave analogously to the near-field for a travelling fire and demonstrate that the firepower (heat release rate) plays an equally important role as the overall fire size in defining the magnitude of the fire-imposed heat fluxes in a large compartment. It is important to highlight that in these experiments, the fire size and HRR are decoupled from each other. These findings show that the low HRRPUA input by the small burner area over the total floor area leads to compartment fire dynamics that are analogous to a travelling fire, in which the rate of energy released into the compartment pales in comparison to fully-developed compartment fires using natural fuels burning over the entire floor area. Consequently, the heat fluxes measured are consistent with the data reported for $V_S/V_{BO} \approx 1$.

4.3. Growing fire experiments

The temporal evolution of the growing fire experiments ($V_S/V_{BO} > 1$) is evaluated by fitting a generalised exponential function to the data to extract the rate of growth of the total gauge heat flux following the approach detailed in Section 3.2.2. This function was found to provide the best fit for experiments exhibiting natural fire growth (i.e. wood cribs). Growth constants (k) for each experiment are shown in Figure 6. Similar to Figure 4, the shaded bars correspond to heat fluxes obtained by transforming gas temperature measurements using the empirical total heat transfer coefficients from Table 2.

The data shows the largest growth rates for the ETFT 11, Vaseli, x-One experiments, which also correspond to the faster flame spread rates observed within each experimental compartment. The lowest growth rate constant is identified from the Malveira Fire Test, which accelerates mildly for over an hour before the ignition of a combustible ceiling that induces a rapid flame spread across the fuel-bed. The enhanced thermal feedback from the flaming ceiling and rapidly descending smoke layer increases the surface flame spread rate, leading to the transition to a fully-developed fire (Gupta *et al.* 2020). To help interpret the growth rates, three values of k are selected from the experimental data and used to illustrate the temporal evolution of the heat flux, also shown in Figure 6. The pre-exponential constant A is simply the initial heat flux for growing fire mode and is set at unity (in solely the figure) to illustrate the effect of the growth constants. The growth constants obtained from the data highlights the large range in the possible temporal evolutions of heat fluxes across the large compartment fire experiments. It is important to note that the inferred ceiling heat fluxes from the exponential function are bounded by the heat flux received at the fuel bed reaching a critical heat flux for rapid flame spread ($\dot{q}''_{rs,crit}$) (Gupta *et al.* 2020). This heat flux is intrinsically linked to the heating of the ceiling, as this energy is used to raise the temperature of the compartment boundaries and smoke layer, thereby increasing the amount of irradiation onto the fuel on the floor. Once the critical threshold $\dot{q}''_{rs,crit}$ is attained at the flame front, the fire will transition to Mode 1 ($V_S/V_{BO} \rightarrow \infty$), and the heat flux will approach quasi-steady conditions. There is insufficient evidence to quantify, in general terms, the relationship of the ceiling to floor heat fluxes as this is geometry and fuel dependent. However, it is clear from this analysis that the growth constants k are consistent with the evolution of the flame spread rate in time. Comparing the timescales to attain rapid flame spread from the data for the ETFT experiments (Gupta *et al.* 2020) and x-One and x-Two (Heidari *et al.* 2020) to the predicted timescales to exceed 100 kW/m^2 from the growth constants k shows these timescales are quite consistent. Past this point, the fires transition to Mode 1. Therefore, the growth rate constant for the heat flux is a good indicator of the flame spread rate. The nature of the transition time to Mode 1 is heavily influenced by the

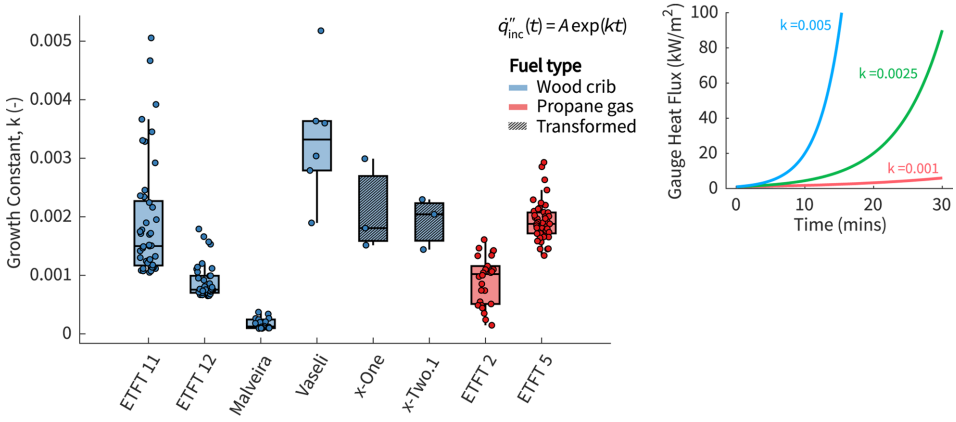


Figure 6. Exponential growth constants of the heat flux data from each growing fire ($V_S / V_{BO} > 1$) experiment. The plot on the side shows the temporal evolution of the heat flux for a range of growth constants obtained from the experimental data assuming that A = 1 kW/m^2.

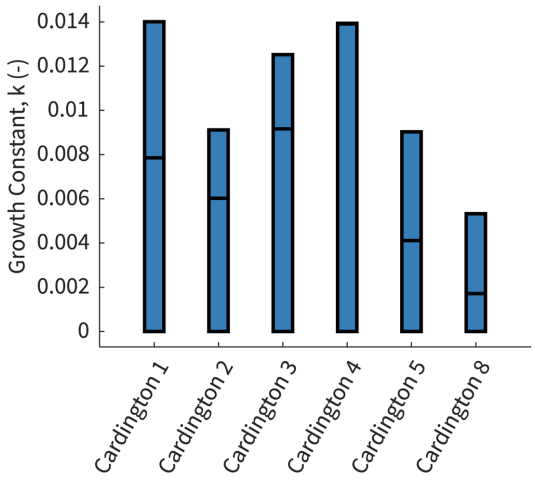


Figure 7. Bar chart detailing the heat flux growth rate constants from the two heat flux meters (indicated by the horizontal black bar) for each of the Cardington experiments. Cardington 6 is omitted from the data as no qualitative or quantitative characterisation of the fire development is provided.

compartment geometry and is exemplified by the growth constants from the results of the Cardington experiments, shown in Figure 7. These experiments have considerably smaller opening areas than those shown in Figure 6.

Growth rates for each of the Cardington experiments (Figure 7) significantly exceed the experiments presented in Figure 6, with the only exception being Cardington 6, which is highly under-ventilated. These rates indicate a particularly incredibly fast flame spread upon ignition, and thus these experiments can be considered as fully-developed. The very fast heating rates are likely associated with a combination of the low thermal inertia of the boundaries and the low ceiling height relative to the crib height. The lining material for each experiment except for Cardington 8 comprises a low-density ceramic fibre. A plasterboard lining is used to encapsulate the boundaries for Cardington 8, which has larger thermal inertia and therefore slower growth constants when compared to Cardington 2, which has almost the same opening factor, indicating that the thermal inertia is an important parameter in defining the growth rate. As there is only one opening, the convective heat losses will be considerably less than the other experiments from Figure 6. Cardington 1 and Cardington 4, which show the largest growth rates, have the same fuel load density of wood crib (40 kg/m^2) and thermal inertia, but different opening sizes. The third-largest growth rate is identified from Cardington 3, which has a fuel load density of 20 kg/m^2 and the same thermal inertia as Cardington 1 and Cardington 4, but with a smaller opening area. The trends highlight the potential for very fast fire development leading to $V_S/V_{BO} \to \infty$ for large compartments under specific fuel and compartment conditions that permit rapid smoke layer development and heating of the gas-phase. This is achieved by a complex combination of parameters that include the fuel load density, ceiling to fuel height ratio, the size of the openings, and the thermal inertia of the linings. There is insufficient data and variability in the available parameter space to quantify the relative importance of the compartment and fuel parameters in defining the compartment flame spread rate and the resultant heat flux growth rates.

5. Conclusions

Tall buildings have transformed modern cities and have driven significant advances in optimisations of building design. Optimisation of fire safety in tall buildings are currently limited by an inadequate understanding of how structures behave when exposed to realistic fire conditions as factors of safety for fire safety provisions cannot be quantified. Our ability to describe the fire dynamics and thermal exposure of large open-plan spaces typical of tall buildings is core to addressing this limitation.

This paper provides a historical overview of compartment fire dynamics and introduces the complexities associated with scaling-up to large open-plan compartments. A review of the state-of-the-art experimental research of large compartment fires from the past three decades is undertaken. Experimental results are collected from almost every compartment fire experiment reported in the literature ($n = 37$) that exhibits the geometric characteristics relevant to the open-plan compartment to quantify the spatial and temporal distributions of ceiling-imposed heat fluxes to elucidate the state-of-the-art of open-plan compartment fire dynamics and current research gaps. It was found that the thermal exposure from the experimental data can be assimilated in terms of the ratio of the flame spread velocity and burnout front velocity (V_S/V_{BO}). Ceiling heat fluxes can be grouped into three distinct modes of V_S/V_{BO}, each which carry a characteristic order of magnitude and temporal distribution.

Fire-imposed heat fluxes are very large for the fully-developed fires where $V_S/V_{BO} \to \infty$ (Mode 1) and can be considered steady-state, with peak mean values distributed within 50 kW/m^2 – 250 kW/m^2 for the experiments involving wood cribs. The wide scatter in the experimental data highlights the complex nature of this fire mode, which results from a complex and unresolved interaction of the compartment geometry, opening sizes, boundary lining materials, fuel type and fuel load densities. The values obtained for the Mode 1 experiments challenge the long-held belief that small under-ventilated or *Regime I* type compartments impose a more onerous thermal loading, in terms of magnitude onto the structure.

Heat fluxes for the travelling fire experiments where $V_S/V_{BO} \approx 1$ (Mode 3) are significantly smaller, peaking at approximately 25 kW/m^2 and 12 kW/m^2 for the near and far-fields, respectively. Similar to the fully-developed

fires, quasi-steady behaviour is assumed, and therefore the spatial distribution of mean near-field and far-field heat fluxes are presented for each experiment. Such low heat fluxes indicate that there is no direct flame impingement of the ceiling, with the resultant ceiling jets in the far-field being quite weak. Consequently, near-field heating is governed by the ratio of the heat release rate of the fire (which transfers heat primarily by convection from the fire plume) and ceiling height. The fuel nature and sooting propensity of the fuel control far-field heating. The heat fluxes obtained from this analysis of the available experimental data are an order of magnitude smaller than current design methods for travelling fires and indicate that the underlying assumptions for travelling fire methods are overly conservative and do not adequately capture the physics of travelling fires and should be revisited.

The temporal evolution of the heat fluxes for the growing fire experiments where $V_S/V_{BO}>1$ (Mode 2) is described through an exponential growth function, with a range of growth constants (accounting for spatial variability) extracted from the data. The transient evolution of heat fluxes is directly related to the flame spread rate of the fuel, and are therefore driven by the coupling of the compartment and fuel properties driven by the coupling of the compartment and fuel properties.

The data assimilated for each mode within the entire set of large compartment fire experiments cover a limited range of compartment and fuel characteristics, and yet, are still extremely scattered. In the absence of systematic testing programmes by concerted research in a similar manner to the original CIB tests, no predictive model to quantify the fire dynamics and thermal exposure based on the compartment and fuel characteristics can be offered. In particular, the dynamics and thermal boundary conditions for fully-developed large compartment fires with larger openings are identified as a major knowledge gap that warrants further study. The data does highlight, however, that the fire-imposed heat fluxes are bounded by V_S/V_{BO} and carry distinct order of magnitudes and temporal distributions, thereby offering a potential pathway to construct a framework to quantify heat fluxes based on real fire scenarios.

Acknowledgments

This work is part of the EPSRC funded *Real Fires for the Safe Design of Tall Buildings* project (Grant: No. EP/J001937/1). Additional funding support was provided from the RFCS funded *TRAFIR* project (Grant No. 754198). We thank all those involved in the large-scale experiments that underpin this paper. In particular, we extend our thanks (in no particular order) to Dr Johan Sjöström, Dr Stephen Welch, Dr Simo Hostikka, Dr Frantisek Wald and Dr Kamila Cabová for assistance in accessing older data sets. We are grateful to Prof. Bart Merci and Prof. Ali Rangwala for their comments on the first author's PhD thesis, which has helped improve this paper. We acknowledge helpful contributions from Ian Pope, Elhalm Saffari and Dr Felix Weisner regarding the data processing and presentation. The thoughts and concepts expressed in this paper have resulted from extensive discussions with numerous individuals over the years, to whom we are truly grateful.

References

Abecassis-Empis, C., Reszka, P., Steinhaus, T., Cowlard, A., Biteau, H., Welch, S., Rein, G. and Torero, J. L. (2008). "Characterisation of Dalmarnock fire Test One", *Exp. Therm. Fluid Sci.*, 32(7), 1334-1343.

Ahmadi, M. T., Aghakouchak, A. A., Shahmari, A., Modares, T., Mirghaderi, R., Tahouni, S., Garivani, S., Shahmari, A. and Epackachi, S. (2020). "Collapse of the 16-Story Plasco Building in Tehran due to Fire", *Fire Technol.*, 56(2), 769-799.

Alpert, R. L. (1972). "Calculation of response time of ceiling-mounted fire detectors", *Fire Technol.*, 8(3), 181-195.

Alpert, R. L. (1975). "Turbulent ceiling-jet induced by large-scale fires", *Combust. Sci. Technol.*, 11(5-6), 197-213.

Behnam, B. (2019). "Fire Structural Response of the Plasco Building: A Preliminary Investigation Report", *Int. J. Civ. Eng.*, 17(5), 563-580.

Bergman, T. L., Lavine, A. S., Incropera, F. P. and DeWitt, D. P. (2011). *Fundamentals of heat and mass transfer.* 7th ed. Hoboken, NJ: Hoboken, NJ: Wiley.

Charlier, M., Vassart, O., Dai, X., Welch, S., Sjöström, J., Anderson, J. and Nadjai, A. (2020). "A simplified representation of travelling fire development in large compartment using CFD analyses", in *Proc. 11th Int. Conf. Struct. Fire*, 526-536.

Clifton, C. G. (1996). *Fire Models for Large Firecells*.

Cooke, G. M. E. (1998). *Tests to Determine the Behaviour of Fully Developed Natural Fires*.

Council on Tall Buildings and Urban Habitat. (2021). *CTBUH Year in Review : Tall Trends of 2020 Tall Buildings in 2020 : COVID-19 Contributes To Dip in Year-On-Year Completions*.

Cowlard, A., Bittern, A., Abecassis-empis, C. and Torero, J. L. (2013). "Some Considerations for the Fire Safe Design of Tall Buildings", *Int. J. High-Rise Build.*, 2(1), 63-77.

Dai, X., Welch, S. and Usmani, A. (2017). "A critical review of 'travelling fire' scenarios for performance-based structural engineering", *Fire Saf. J.*, 91, 568-578.

Dai, X., Welch, S., Vassart, O., Cábová, K., Jiang, L., Maclean, J., Clifton, G. C. and Usmani, A. (2020). "An extended travelling fire method framework for performance-based structural design", *Fire Mater.*, 44(3), 437-457.

Drysdale, D. (2011). *An Introduction to Fire Dynamics*. 3rd edn. Wiley.

Engelhardt, M. D. M. D., Meacham, B., Kodur, V., Kirk, A., Park, H., Straalen;, van Straalen, I., Maljaars, J., van Weeren, K., De Feijter, R. and Both, K. (2013). "Observations from the Fire and Collapse of the Faculty of Architecture Building, Delft University of Technology", in *Struct.*

Congr. 2013. ASCE Pittsburgh, 1-12.

Eurocode 1: Actions on structures - Part 1-2: General actions - Actions on structures exposed to fire. (2002). *EN 1991-1-2*. CEN Brussels.

Fernandez-Pello, A. C. and Hirano, T. (1983). "Controlling mechanisms of flame spread", *Combust. Sci. Technol.*, 32(1-4), 1-31.

Finney, M. A., Cohen, J. D., Forthofer, J. M., McAllister, S. S., Gollner, M. J., Gorham, D. J., Saito, K., Akafuah, N. K., Adam, B. A., English, J. D. and Dickinson, R. E. (2015). "Role of buoyant flame dynamics in wildfire spread", *Proc. Natl. Acad. Sci. U. S. A.*, 112(32), 9833-9838.

Fletcher, I. A. 1; Welch, S., Alvear, D., Lazaro, M., Capote, J. A. A., Alvear, ; and Lázaro, ; (2007). "Model-based analysis of a concrete building subjected to fire", in *Proc. 4th Int. Work. Structures Fire*, 779-790. Available at: https://era.ed.ac.uk/handle/1842/1988.

Gales, J. (2014). "Travelling Fires and the St. Lawrence Burns Project", *Fire Technol.*, 50(6), 1535-1543.

Gales, J., Chorlton, B. and Jeanneret, C. (2021). "The Historical Narrative of the Standard Temperature-Time Heating Curve for Structures", *Fire Technol.* Springer, 529-558.

Gamba, A., Charlier, M. and Franssen, J.-M. (2020). "Propagation tests with uniformly distributed cellulosic fire load", *Fire Saf. J.*, 117(103213), 1-11.

Gann, R. G. (2005). *Reconstruction of the fires in the world trade center towers*, *NIST NCSTAR*.

Gillie, M., Usmani, A., Rotter, M. and O'Connor, M. (2001). "Modelling of heated composite floor slabs with reference to the Cardington experiments", *Fire Saf. J.*, 36(8), 745-767.

Gillie, M., Usmani, A. S. and Rotter, J. M. (2001). "A structural analysis of the first Cardington test", *J. Constr. Steel Res.*, 57(6), 581-601.

Gross, D. and Robertson, A. F. (1965). "Experimental fires in enclosures", *Symp. Combust.*, 10(1), 931-942.

Gupta, V. (2021). *Open-plan compartment fire dynamics*. The University of Queensland.

Gupta, V., Hidalgo, J. P., Cowlard, A., Abecassis-Empis, C., Majdalani, A. H., Maluk, C. and Torero, J. L. (2021). "Ventilation effects on the thermal characteristics of fire spread modes in open-plan compartment fires", *Fire Saf. J.*, 120(103072), 1-9.

Gupta, V., Maluk, C., Torero, J. L. and Hidalgo, J. P. (2019). "Analysis of Convective Heat Losses in a Full-scale Compartment Fire Experiment", in *Proc. 9th Int. Semin. Fire Explos. Hazards*, 490-501.

Gupta, V., Osorio, A. F., Torero, J. L. and Hidalgo, J. P. (2020). "Mechanisms of flame spread and burnout in large enclosure fires", *Proc. Combust. Inst.*, 38(3), 4525-4533.

Gupta, V., Torero, J. L. and Hidalgo, J. P. (2021). "Burning dynamics and in-depth flame spread of wood cribs in large compartment fires", *Combust. Flame*, 228, 42-56.

Häggkvist, A., Sjöström, J. and Wickström, U. (2013). "Using plate thermometer measurements to calculate incident heat radiation", *J. Fire Sci.*, 31(2), 166-177.

Harmathy, T. Z. (1972). "A new look at compartment fires, Part I", *Fire Technol.*, 8, 196-217.

Heidari, M., Kotsovinos, P. and Rein, G. (2019). "Flame extension and the near field under the ceiling for travelling fires inside large compartments", *Fire Mater.*, 44(3), 421-436.

Heidari, M., Rackauskaite, E., Bonner, M., Christensen, E., Morat, S., Mitchell, H., Kotsovinos, P., Turkowski, P., Wegrzynski, W., Tofilo, P. and Rein, G. (2020). "Fire experiments inside a very large and open-plan compartment: x-TWO", in *11th Int. Conf. Struct. Fire*, 479-491.

Hidalgo-Medina, J. P. and Hidalgo, J. P. (2015). *Performance-Based Methodology for the Fire Safe Design of Insulation Materials in Energy Efficient Buildings*. The University of Edinburgh.

Hidalgo, J. P., Cowlard, A., Abecassis-Empis, C., Maluk, C., Majdalani, A. H., Kahrmann, S., Hilditch, R., Krajcovic, M. and Torero, J. L. (2017). "An experimental study of full-scale open floor plan enclosure fires", *Fire Saf. J.*, 89, 22-40.

Hidalgo, J. P., Goode, T., Gupta, V., Cowlard, A., Abecassis-Empis, C., Maclean, J., Bartlett, A. I., Maluk, C., Montalvá, J. M., Osorio, A. F. and Torero, J. L. (2019). "The Malveira fire test: Full-scale demonstration of fire modes in open-plan compartments", *Fire Saf. J.*, 108 (102827).

Hidalgo, J. P., Maluk, C., Cowlard, A., Abecassis-Empis, C., Krajcovic, M. and Torero, J. L. (2017). "A Thin Skin Calorimeter (TSC) for quantifying irradiation during large-scale fire testing", *Int. J. Therm. Sci.*, 112, 383-394.

Horová, K., Jána, T. and Wald, F. (2013). "Advances in Engineering Software Temperature heterogeneity during travelling fire on experimental building", *Adv. Eng. Softw.*, 62-63, 119-130.

Ingason, H. and Wickström, U. (2007). "Measuring incident radiant heat flux using the plate thermometer", *Fire Saf. J.*, 42(2), 161-166.

Ingberg, S. H. (1928). "Tests of the Severity of Building Fires", *Q. Natl. Fire Prot. Assoc.*, 22, 43-61.

International Organization for Standardization. (1999). "ISO 834-1:1999, Fire-resistance tests -- Elements of building construction -- Part 1: General requirements".

Jahn, W., Rein, G. and Torero, J. L. (2011). "A posteriori modelling of the growth phase Dalmarnock Fire Test One", *Build. Environ.*, 46, 1065-1073.

Jowsey, A. (2006). *Fire Imposed Heat Fluxes for Structural Analysis*. The University of Edinburgh.

Jowsey, A., Rein, G., Abecassis-empis, C., Cowlard, A. and Reszka, P. (2007). "An analytical approach to define surface heat fluxes to structural members in post-flashover fires", in *Proc. 5th Int. Semin. Fire Explos. Hazards*. Edinburgh: The University of Edinburgh, 692-701.

Kawagoe, K. (1958). *Fire behaviour in rooms*, *Rep. Build. Res. Inst.*

Khan, A. A., Usmani, A. and Torero, J. L. (2021). "Evolution of fire models for estimating structural fire-resistance", *Fire Saf. J.*, 124, 103367.

Killick, R., Fearnhead, P. and Eckley, I. A. (2012). "Optimal detection of changepoints with a linear computational cost", *J. Am. Stat. Assoc.*, 107(500), 1590-1598.

Kirby, B. R., Wainman, D. E., Tomlinson, L. N., Kay, T. R.

and Peacock, B. N. (1994). *Natural Fires in Large Scale Compartments, A British Steel Technical, Fire Research Station Collaborative Project*.

Kirby, B. R., Wainman, D. E., Tomlinson, L. N., Kay, T. R. and Peacock, B. N. (1999). "Natural Fires in Large Scale Compartments", *Int. J. Eng. Performance-Based Fire Codes*, 1(2), 43-58.

Law, A. and Bisby, L. (2020). "The rise and rise of fire resistance", *Fire Saf. J.*, 116, 103188.

Law, A., Stern-Gottfried, J., Gillie, M. and Rein, G. (2011). "The influence of travelling fires on a concrete frame", *Eng. Struct.*, 33(5), 1635-1642.

Law, M. (1971). *A relationship between fire grading and building design and contents - FRS No. 877*, *Fire Res. Note*.

Law, M. (1983). "Basis for the Design of Fire Protection of Building Structures", *Struct. Eng.*, 61 A(1), 25-33.

Law, M. and O'Brien, T. (1989). *Fire safety of bare external structural steel*. The Steel Construction Institute.

Lennon, T. (1998). "Large Compartment Fire Tests on a Full-Scale Eight Storey Building", in *ASTM Spec. Tech. Publ. 1336*, 55-70.

Lennon, T. and Moore, D. (2003). "The natural fire safety concept - Full-scale tests at Cardington", *Fire Saf. J.*, 38(7), 623-643.

Majdalani, A. H., Cadena, J. E., Cowlard, A., Munoz, F. and Torero, J. L. (2016). "Experimental characterisation of two fully-developed enclosure fire regimes", *Fire Saf. J.*, 79, 10-19.

Maluk, C., Linnan, B., Wong, A., Hidalgo, J. P., Torero, J. L., Abecassis-Empis, C. and Cowlard, A. (2017). "Energy distribution analysis in full-scale open floor plan enclosure fires", *Fire Saf. J.*, 91, 422-431.

Masson, L. (2003). *The Use of an Instrumented Steel Billet to Measure Incident Heat Flux*. MSc Thesis. University of Ulster.

McCaffrey, B. J., Quintiere, J. G. and Harkleroad, M. F. (1981). "Estimating room temperatures and the likelihood of flashover using fire test data correlations", *Fire Technol.*, 17(2), 98-119.

Nadjai, A., Alam, N., Charlier, M., Vassart, O., Dai, X., Franssen, J. and Sj. (2020). "Travelling fire in full scale experimental building subjected to open ventilation conditions", in *Proc. 11th Int. Conf. Struct. Fire*. Brisbane: The University of Queensland, 439-450.

Pchelintsev, A., Hasemi, Y., Wakarnatsu, T. and Yokobayashi, Y. (1997). "Experimental And Numerical Study On The Behaviour Of A Steel Beam Under Ceiling Exposed To A Localized Fire", *Fire Saf. Sci.*, 5(m), 1153-1164.

PIT Project: Behaviour of steel framed structures under fire conditions. Main Report. (2000).

Prahl, J. and Emmons, H. W. (1975). "Fire induced flow through an opening", *Combust. Flame*, 25(C), 369-385.

Rackauskaite, E., Hamel, C., Law, A. and Rein, G. (2015). "Improved Formulation of Travelling Fires and Application to Concrete and Steel Structures", *Structures*, 3, 250-260.

Rackauskaite, E., Kotsovinos, P., Jeffers, A. and Rein, G. (2017). "Structural analysis of multi-storey steel frames exposed to travelling fires and traditional design fires", *Eng. Struct.*, 150, 271-287.

Rein, G., Zhang, X., Williams, P., Hume, B., Heise, A., Jowsey, A., Lane, B. and Torero, J. L. (2007). "Multi-Storey Fire Analysis for High-Rise Buildings", in *11th Interflam*, 605-616.

Rush, D., Dai, X. and Lange, D. (2020). "Tisova Fire Test - fire behaviours and lessons learnt", *Fire Saf. J.*, 103261.

Sanad, A. M., Lamont, S., Usmani, A. S. and Rotter, J. M. (2000). "Structural behaviour in fire compartment under different heating regimes — Part 1 (slab thermal gradients)", *Fire Saf. J.*, 35(2), 99-116.

Sanad, A. M., Lamont, S., Usmani, A. S. and Rotter, J. M. (2000). "Structural behaviour in fire compartment under different heating regimes — part 2: (slab mean temperatures)", *Fire Saf. J.*, 35(2), 117-130.

SFPE Engineering Standard on Calculating Fire Exposures to Structures. (2011). Society of Fire Protection Engineers.

Shorter, G. W. (1959). *St. Lawrence Burns: general report*. Ottowa.

Sjostrom, J., Hallberg, E., Kahl, F., Temple, A., Welch, S., Dai, X., Gupta, V., Lange, D. and Hidalgo, J. (2019). *Characterization of TRAvelling FIRes in large compartments*.

Stern-Gottfried, J. and Rein, G. (2012). "Travelling fires for structural design-Part I: Literature review", *Fire Saf. J.*, 54, 74-85.

Stern-Gottfried, J. and Rein, G. (2012). "Travelling fires for structural design-Part II: Design methodology", *Fire Saf. J.*, 54, 96-112.

Stern-Gottfried, J., Rein, G., Bisby, L. A. and Torero, J. L. (2010). "Experimental review of the homogeneous temperature assumption in post-flashover compartment fires", *Fire Saf. J.*, 45(4), 249-261.

The SFPE Task Group on Fire Exposures to Structural Elements. (2004). *SFPE Engineering Guide on Fire Exposures to Structural Elements*.

Thomas, I., Moinuddin, K. and Bennetts, I. (2005). "Fire development in a deep enclosure", in *Proc. 8th Int. Symp. Fire Saf. Sci.*, 1277-1288.

Thomas, P. H. (1973). "Behavior of fires in enclosures-Some recent progress", *Symp. Combust.*, 14(1), 1007-1020.

Thomas, P. H., Heselden, A. J. and Law, M. (1967). *Fully-developed Compartment Fires: Two Kinds of Behaviour*, *Fire Res. Tech. Pap. No. 18*. H.M. Stationery Office.

Thomas, P. H. and Heselden, A. J. M. (1962). "Behaviour of fully developed fire in an enclosure", *Combust. Flame*, 6(C), 133-135.

Thomas, P. H. and Heselden, A. J. M. (1972). *Fully Developed Fires in Single Compartments*.

Torero, J. L. (2013). "Scaling-Up fire", *Proc. Combust. Inst.*, 34(1), 99-124.

Torero, J. L. (2016). "Flaming Ignition of Solid Fuels", in *SFPE Handb. Fire Prot. Eng.* New York: Springer, New York, NY, 633-661.

Torero, J. L., Law, A. and Maluk, C. (2017). "Defining the thermal boundary condition for protective structures in fire", *Eng. Struct.*, 149, 104-112.

Torero, J. L., Majdalani, A. H., Abecassis-Empis, C. and Cowlard, A. (2014). "Revisiting the compartment fire", in *Proc. 11th Int. Symp. Fire Saf. Sci.*, 28-45.

Usmani, A. S., Rotter, J. M., Lamont, S., Sanad, A. M. and Gillie, M. (2001). "Fundamental principles of structural behaviour under thermal effects", *Fire Saf. J.*, 36(8), 721-744.

Wakamatsu, T., Hasemi, Y., Kagiya, K. and Kamikawa, D. (2003). "Heating mechanism of unprotected steel beam installed beneath ceiling and exposed to a localized fire: Verification using the real-scale experiment and effects of the smoke layer", *Fire Saf. Sci.*, 1099-1110.

Welch, S., Jowsey, A., Deeny, S., Morgan, R. and Torero, J. L. (2007). "BRE large compartment fire tests-Characterising post-flashover fires for model validation", *Fire Saf. J.*, 42(8), 548-567.